

RESEARCH

Open Access



# Early recovery of leukocyte subsets is associated with favorable progression-free survival in patients with inoperable stage II/III NSCLC after multimodal treatment: a prospective explorative study

Thomas P. Hofer<sup>1\*</sup> , Alexander E. Nieto<sup>2</sup>, Lukas Käsmann<sup>2,3,5</sup>, Carolyn J. Pelikan<sup>1</sup>, Julian Taugner<sup>2</sup>, Saloni Mathur<sup>1</sup>, Chukwuka Eze<sup>2</sup>, Claus Belka<sup>2,3,4,5</sup>, Farkhad Manapov<sup>2,3,5†</sup> and Elfriede Noessner<sup>1†</sup> 

## Abstract

**Background** We explored the dynamic changes of major leukocyte subsets during definitive treatment of patients with inoperable stage II/III NSCLC lung cancer and correlated it to survival to identify subpopulations associated with maximal patient benefit.

**Methods** We analyzed peripheral blood of 20 patients, either treated with thoracic radiotherapy (RT), concurrent chemo-radiotherapy (cCRT), or cCRT with additional immune-checkpoint inhibition therapy. Peripheral blood of 20 patients was collected at 9 timepoints before, during, and up to 1 year post treatment and analyzed by multi-color flow cytometry. Statistical analysis was conducted for leukocyte subpopulations, IL-6, progression-free survival (PFS) and overall survival (OS).

**Results** Increase of absolute lymphocyte counts (ALC) after the end of RT until 6 months thereafter was a predictor of PFS. Baseline lymphocyte counts showed no significant correlation to PFS or OS. Early recovery of absolute counts (AC) at 3 weeks after RT, total CD3+T-cells, and CD8+ cytotoxic T-cells distinguished those patients with favorable PFS ( $\geq 12$  months) from all other patients. Discriminant analysis identified B-cells, neutrophil-lymphocyte-ratio (NLR), CD4+T-helper-cells, and NK-cells as predictors of favorable PFS. High variability in IL-6 plasma concentration of consecutive measurements within 6 months after the end of RT correlated negatively with PFS.

**Conclusion** Our results suggest that two parameters commonly assessed in clinical routine can be used to predict patient outcome. These are: early increase in CD8+ T-cell lymphocyte count and variability in IL-6 plasma

<sup>†</sup>Farkhad Manapov and Elfriede Noessner contributed equally to this work.

\*Correspondence:  
Thomas P. Hofer  
thomas.hofer@helmholtz-munich.de

Full list of author information is available at the end of the article



concentration, that are correlated to patients with favorable, respectively, poor outcome after definitive therapy independent of treatment regimen.

**Keywords** Non-small cell lung cancer, Linear discriminant analysis, Peripheral blood markers, Area under curve analysis, Immune checkpoint therapy, Progression-free survival, Overall survival, CD4+ T-cells, CD8+ T-cells, NK-cells, B-cells, Neutrophils, Eosinophils

## Background

Non-small cell lung cancer (NSCLC) accounts for approximately 85% of all lung cancers, and prognosis remains poor with a low 5-year survival rate, only up to 36% of patients with an advanced stage experiencing sustained clinical benefit from therapy [1]. Treatment advances were achieved by introducing immune checkpoint therapy (ICI) as monotherapy or in addition to chemo-radiotherapy [2, 3].

There is a medical need to not only find more effective therapies but also to identify those patients who are likely to benefit from added ICI or should be spared the side effects if ICI is ineffective [4]. Ongoing efforts are being made to identify suitable biomarkers to predict benefit or non-response, preferably obtained from easily and repeatedly accessible biomaterial like venous peripheral blood.

Leukocytes are targets of irradiation when circulating through the lung. It is well known that lymphopenia occurs during radiation therapy that is linked with patient's outcome [5, 6], and may affect subsequent ICI therapy [7]. It is therefore important to know which lymphocyte sub-population can indicate rapid recovery and could therefore serve as a biomarker for clinical outcome and treatment allocation.

In this prospective single-center study we aimed to explore whether the dynamics of defined lymphocyte subsets might be suitable to predict survival. We performed immune monitoring on patients who underwent therapy for inoperable stage II/III NSCLC. We prospectively report on characteristics of absolute T-cell counts (total CD3+ T-cells, CD3+CD4+, and CD3+CD8+ T-cells), B-cells, NK-cells, neutrophils, eosinophils, and IL-6 plasma levels regarding patient treatment and outcome (PFS, and OS).

## Materials and methods

### Patients, controls, blood sampling, treatment

Blood samples from patients with unresectable stage II/III non-small cell lung cancer (NSCLC; 8th TNM staging system) without distant metastases were obtained before as well as during treatment and follow-up at the Clinic for Radiation Oncology of the LMU University Hospital, Munich. All patients were included in this study on a voluntary basis and provided written informed consent. Approval has been granted by the Human Ethics Committee of the Ludwig-Maximilians-University of Munich

reference no. 17–632 and research was conducted in accordance with the Declaration of Helsinki.

Twenty patients (17 male, 3 female), first diagnosed with a median age of 65.5 years (range 34 to 79) were enrolled in this study (Table 1; Fig. S1). Blood samples were collected before onset of therapy (A.1 at week 0), twice during (A.2 and A.3 at week 2 and 5, respectively) and at the end of radiotherapy (RTend at week 7), and during follow up (C.1 to C.5 at week 10, 20, 35, 48, and 60) (Fig. 1, Fig. S1). The controls were 9 apparently healthy individuals (CTRL) with a median age of 30 years (range 24 to 59) at the timepoints of blood sampling; 1 male and 8 females (Fig. 2; Table 1). Samples were processed and analyzed simultaneously and identically to the patient samples.

Patient treatment modality was concluded at the discretion of the treating physician based on clinical standards and following multidisciplinary tumor board discussion. Tab. S1 provides information regarding tumor volume, radiation dose regimens, radiation modalities, and chemo therapeutics. Image guided radiation therapy, motion characterization, PET-based target contouring was used to arrange radiation therapy treatment. Two patients received RT alone, 18 patients were treated with platinum-based concurrent cCRT, and 7 patients received additional ICI either concurrently (nivolumab) or sequentially (durvalumab). Details are provided in Fig. S1.

### Leukocyte phenotyping

Blood was collected using 3 K-EDTA S-Monovette tubes (Sarstedt, Germany) and samples were analyzed within 3 h. Using 100 µl of whole blood, erythrocytes were lysed, cells were surface-stained, spiked with counting beads (Flow-Count Fluorospheres, Beckman Coulter, Germany) and analyzed on a BD LSRII flow cytometer equipped with Diva Software (version 8).

To identify immunocyte subpopulations, leukocytes were gated within FSC-A vs. SSC-A to exclude debris using FlowJo Software (version 10). T-cells were defined as CD3+CD14- CD16- CD19/20- single cells (FSC-A vs. FSC-H) and subsequently subdivided into CD4+ and CD8+ T-cell populations (Fig. S2). B-cells were identified as CD19/20+CD14- CD56- CD16- single cells. For NK-cells, highly CD16-positive (neutrophils), CD3+, CD19+20+, and CD14+ cells were excluded, and the remaining single cells cell population was gated for

**Table 1** Characteristics of patients with NSCLC and healthy controls

Patients	<i>n</i> =20
Age (mean, SD) (years)	62.5 ± 13.75
(median / range) (years)	65.5 / 34-79
Sex (male / female)	17 / 3
Adenocarcinoma	11
Squamous cell carcinoma	8
Undiff. NSCLC	1
Therapy (RT / cCRT / cCRT-ICI / salvage therapy)	2 / 12 / 7 / 3
Initial UICC Stage (IIB / IIIA / IIIB / IIIC)	2 / 5 / 8 / 5
Initial CRP (mean, SD) (mg/L)	3.33 ± 5.72
(median / range) (mg/L)	0.4 / 0.1 - 22.4
Initial LDH (mean, SD) (U/L)	277.2 ± 121.7
(median / range) (U/L)	250 / 166 - 751
Initial Karnofsky Score (60 / 70 / 80 / 90 / 100)	1 / 1 / 4 / 6 / 8
Pneumonitis (CTAE Grade 0 / 1 / 2 / 3)	5 / 4 / 9 / 2
Survival (< 1y / ≥ 1 < 2y / ≥ 2 < 3y / ≥ 3y < 4y / ≥ 3y < 4y / ≥ 5)	3 / 5 / 1 / 2 / 1 / 8
Allergies	1 (garlic)
Developed distant metastasis	8
Local remission	9
Smokers (none / active / ex)	1 / 7 / 12
Smoking history > 50 pack years (patients)	8
Healthy Controls	<i>n</i> =9
Age (mean, SD) (years)	35 ± 13.74
(median / range) (years)	30 / 24-59
Sex (male / female)	1 / 8
Smokers (none / active / ex)	8 / 1 / 0

CD56+ CD16+. Flow-Count counting beads (Beckman Coulter) were gated within FSC-A vs. SSC-A and subsequent event count was determined within 695 nm emission channel (PerCP-Cy5.5) vs. SSC-H dot plot. Total CD3+ T-cells include CD3+ CD4+ and CD3+ CD8+ cell counts, and lymphocytes include T-cell, B-cell, and NK-cell counts. For more detailed information, please refer to the supplementary materials.

Further details on sample preparation, staining, gating strategy, and cell type identification are given in the

supplements (Fig. S2, Tab. S2). Neutrophil and eosinophil counts were obtained from clinical routine blood testing (clinical chemistry) using a Symex XN-1000 System (Sysmex, Kobe, Japan). Neutrophil and lymphocyte counts were used to calculate Neutrophil-Lymphocyte-Ratio (NLR).

#### Analysis of immunocyte population dynamics and variation of IL-6 plasma concentration

The absolute lymphocyte count (ALC) represents the absolute cell number of a particular immune cell subset for each patient at each time point. Stratified by PFS category, this provides insight into the potential contribution that the cell number of a particular subset at a specific time point might have to the patient outcome. The ALC at specified time points, however, neglects the dynamic changes that occur during a time period.

To picture the dynamic processes during this phase between RTend - C.3 (6 months after treatment end), the area under the curve (AUC) of the absolute cell counts of the major leukocyte subpopulations was calculated. It is conceivable that the absolute cell count at one time point has no association to e.g., PFS. However, if this absolute value is achieved through an increase from a previously low value (e.g., dynamic increase) it might be meaningfully associated with PFS. Low or high AUC reflects higher or lower ALC in this period.

Serum IL-6 levels were quantified using the Elecsys IL-6 immunoassay on the Cobas e401 clinical chemistry analyzer (Roche Diagnostics, Mannheim, Germany). Measurements were consistent throughout the entire study period.

#### Statistical analysis

This study was designed as a discovery study with the intention of generating hypotheses. Statistical tests were Student's t-test, Kruskal Wallis test, Spearman's correlation test, Log-rank (Mantel-Cox), Fisher's Exact test, and

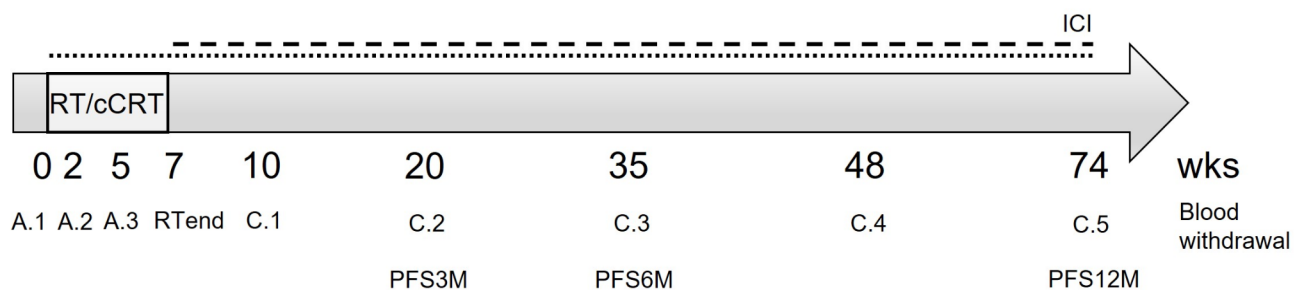


**Fig. 1** Overview of the study design. Blood samples were collected before (A.1), during and at the end of radio- or concurrent radio-chemo-therapy (RT or cCRT; A.2, A.3, RTend), as well as up to one year after end of therapy (C.1 to C.5). Patients undergoing additional ICI therapy either received Nivolumab (...) concurrent to cCRT or Durvalumab sequential to cCRT (- - -), with continuation for up to one year. PFS assessment started with completion of cCRT (time point RTend). PFS3M refers to PFS until 3 months after RTend, PFS6M is PFS up to 6 months and PFS12M PFS up to 12 months after RTend. Detailed information on the patients' individual treatment regimen is summarized in Figure S1

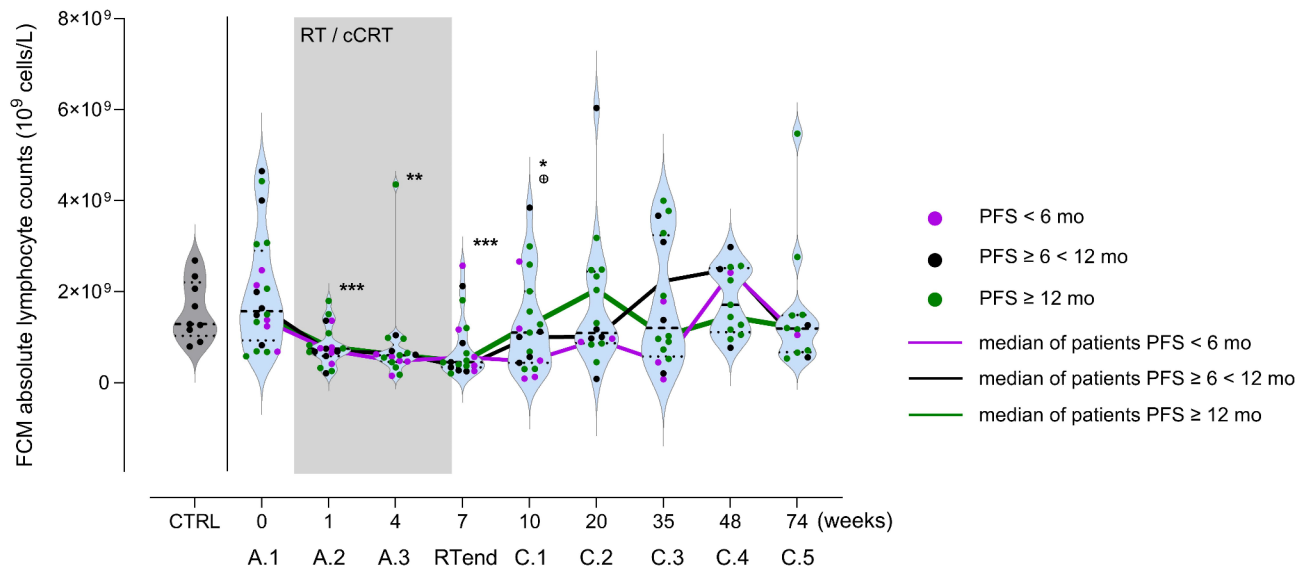


**Fig. 2** ALC in NSCLC patients' peripheral blood ( $n=20$ ) before (A.1), during (A.2, A.3, RTend), and up to 1 y (C.1-C.5) after treatment. Grey violin represents ALC of CTRL ( $n=9$ ). Each dot represents an individual, color codes the PFS group of the patients. Grey area represents the interval of radio- (RT) or chemoradiotherapy (cCRT), color-coded lines connect the median of ALC of each PFS group at the different timepoints. The bold dashed line in the violins indicate median, light dotted lines the lower and upper quartile. Student's t test, \*  $p < 0.05$ , \*\*  $p < 0.01$ , \*\*\*  $p < 0.001$  compared to A.1; ⊕  $p < 0.05$  compared to preceding timepoint

Log-Rank for trend. Differences were considered significant with  $p < 0.05$ .

For analysis of variation of IL-6 concentration during RTend-C.3, standard deviation of absolute values at the consecutive time points RTend, C.1, C.2, and C.3 were calculated and stratified according to groups with poor ( $< 6$  months), intermediate ( $\geq 6 < 12$  months), and favorable ( $\geq 12$  months) PFS.

Unsupervised clustering groups data into clusters based on their similarity, without needing prior information, if and how the data would be related. This approach helps in exploring the data and identifying patterns without introducing bias based on assumed prior knowledge.

Linear discriminant analysis (LDA) is a statistical method used for dimensionality reduction and classification. It aims to find linear combinations of features, here the predictor variables (e.g. absolute cell counts of the blood cell subsets), that best separate two or more classes, here the three PFS categories. Separation of the classes is achieved by maximizing the ratio of the between-class and the within-class variance. This results in a projection indicating which and how strongly the predictor variables contribute to separate the respective class. The projection is visualized by an arrow of a given direction and length [8, 9].

For heatmap visualization and linear discriminant analysis (LDA), R statistical software V4.2.1 and the packages ComplexHeatmap V2.12.1, Dplyr V1.0.10, Plyr V1.8.7, missMDA V1.18, Openxlsx V4.2.5, Stats V4.3.0 and Tidyverse 1.3.2 were used. Further packages for LDA were ggord from Marcus W. Beck (2017), ggord: Ordination

Plots with ggplot2. R package version 1.0.0, <https://zenodo.org/badge/latestdoi/35334615>. For generating graphs and Kaplan-Meier curves, GraphPad Prism V9, and for MANOVA analysis Past V4.11 [10] were used.

## Results

### No prognostic value of ALC for PFS or OS at any single timepoint before, during and after treatment

Baseline ALC were highly heterogenous in the NSCLC patient cohort ( $n=20$ ) with a higher median of  $1.57$  (range  $4.65-0.58$ )  $10^9$  cells/L of ALC compared to the controls ( $n=9$ , median  $1.29$ , range  $2.69-0.80$ )  $10^9$  cells/L). All patients experienced moderate to severe lymphocytopenia (assessed per the Common Terminology Criteria for Adverse Events v5.0) during RT/cCRT with median ALC of  $0.75$  (range  $1.80-0.21$ ),  $0.61$  (range  $4.36-0.15$ ), and  $0.46$  (range  $2.57-0.21$ )  $10^9$  cells/L at timepoint A.2, A.3, and RTend, respectively (grey area in Fig. 2). ALC recovered after RTend reaching median values of  $1.10$  (range  $3.85-0.09$ )  $10^9$  cells/L at C.1 (3 wks after RTend),  $1.09$  (range  $6.04-0.09$ )  $10^9$  cells/L at C.2 (3 mo after RTend),  $1.21$  (range  $4.00-0.08$ )  $10^9$  cells/L at C.3 (6 months after RTend),  $1.72$  (range  $2.99-0.77$ )  $10^9$  cells/L at C.4 (10 mo after RTend), and  $1.19$  (range  $5.47-0.54$ )  $10^9$  cells/L at C.5 (13 mo after RTend). The recovery varied across patients, some with poor others with good increase in cell counts.

Patients were stratified according to PFS after RTend, with poor PFS  $< 6$  months indicated by purple dots, intermediate PFS  $\geq 6 < 12$  months shown as black dots, and favorable PFS  $\geq 12$  months depicted as green dots.

Patients with favorable PFS had on average an early increase in ALC within 3 weeks after RTend (C.1), peaking at timepoint C.2 (14 weeks after RTend) and return to a median ALC comparable to the CTRL. Patients with poor and intermediate PFS had a delayed increase in ALC with a peak in cell counts at C.4 (40 weeks). Although these data indicated that an early recovery of ALC may be beneficial with regards to PFS, there was high ALC heterogeneity within the PFS groups: 3 of 6 patients in the favorable PFS group had no early ALC peak at 14 weeks.

#### Dynamics of leukocyte subpopulations after RT

Favorable PFS group ( $\geq 12$  months) showed significant increase in AC from RTend to C.1 for lymphocytes, total T-cells, and CD8+ T-cells. For the other PFS groups, lymphocytes and CD4+ T-cells did not increase, or the increase occurred later (between RTend and C.3) (Fig. 3, Fig. S4). This was observed for total lymphocytes as well as total CD3+ T-cells and CD8+ T-cells, but not for CD4+ T-cells (for medians and p-values see Tab S3). This implies that an early increase of lymphocytes, total CD3+ T-cells, or CD8+ T-cells within 3 or 14 weeks after

RTend (C.1, or C.2) identifies patients with a favorable progression-free survival-time  $\geq 12$  months.

An increase in neutrophil count with inadequate T-cell and no NK-cell expansion after RTend was observed in the poor prognostic group (Fig. 3, Fig. S4). The intermediate and favorable prognostic groups showed peripheral NK-cell increase after RTend (Fig. S4) while the poor prognostic group did not (median value for intermediate group at RTend 0.014, at C.1 0.040, at C.2 0.132, at C.3 0.257  $10^9$  cells/L; RTend-C.1  $p=0.094$ , RTend-C.2  $p=0.011$ , RTend-C.3  $p=0.015$ ; median value for favorable group see Tab. S3). The favorable prognostic group showed increase after RTend of CD8+ T-cells (median value for intermediate group at RTend 0.14, at C.1 0.51, at C.2 0.42, at C.3 0.73  $10^9$  cells/L; RTend-C.1  $p=0.0596$ , RTend-C.2  $p=0.053$ , RTend-C.3  $p=0.031$ ; median value for favorable group, Tab. S3).

All patients experienced leukocytopenia following RT or cCRT (Fig. 2). We hypothesized that the change of lymphocytes within the first 6 months after end of therapy might be most meaningful for therapy response as the immune system reconstitutes and can react to

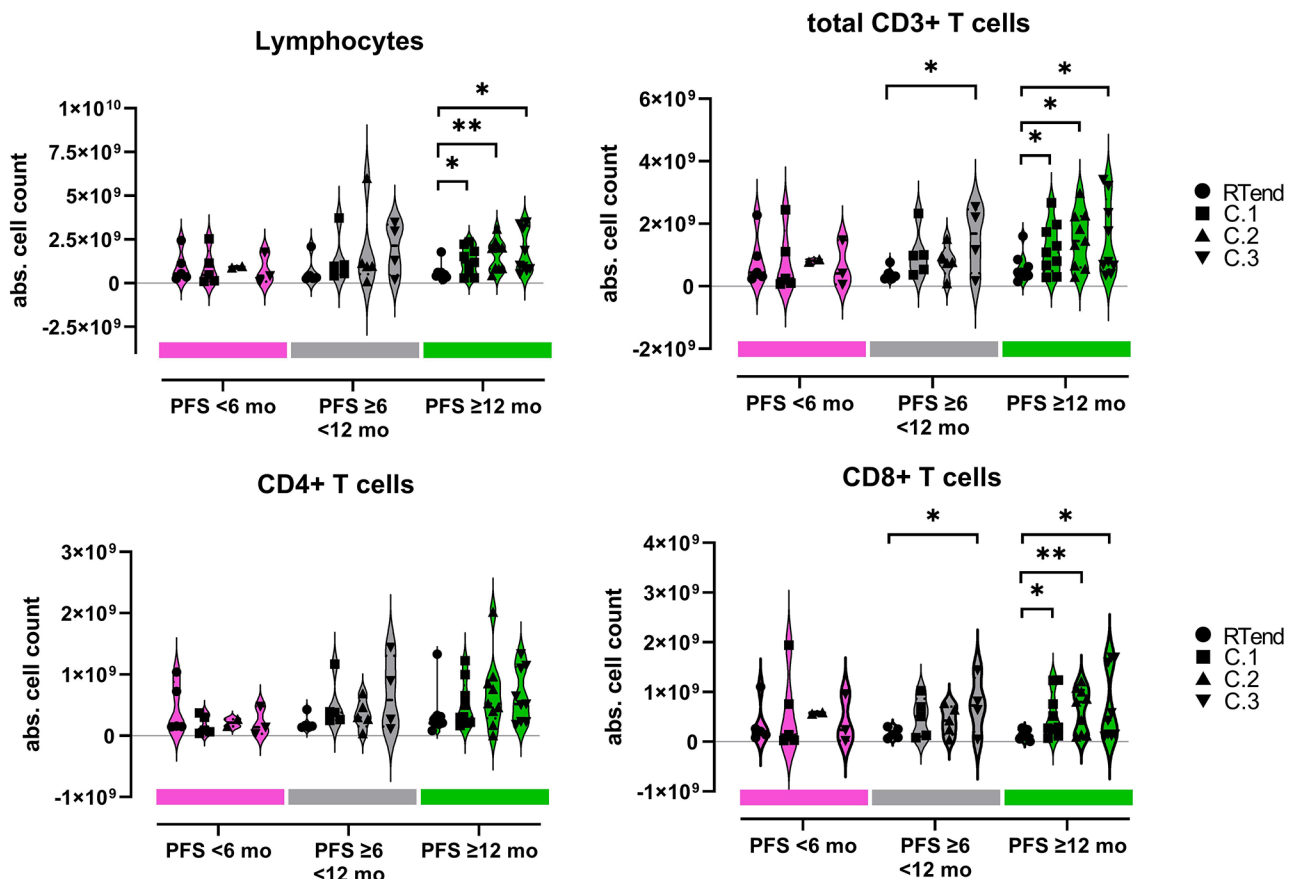


**Fig. 3** Absolute cell counts of lymphocytes, CD3+T-cells, CD4+T-cells, and CD8+T-cells (analyzed with flow cytometry) at timepoints RTend, C.1, C.2, and C.3 within the different PFS groups (PFS <6 months (red), PFS  $\geq 6 < 12$  months (grey), PFS  $\geq 12$  months (green)). Cell counts were derived from flow cytometry (gating strategy in Fig. S2), each dot represents an individual. Comparison was performed across timepoints within each PFS groups, bold dashed line in the violins indicate median, light dotted lines lower and upper quartile. Student's t-test, \*  $p < 0.05$ , \*\*  $p < 0.01$

neoantigens released from destroyed tumor cells. To picture the dynamic processes during this phase between RTend-C.3 (6 months), AUC of the absolute cell counts of the major leukocyte subpopulations was calculated and compared to patient outcome.

Higher AUC for the period between RTend-C.3 reflect a more pronounced increase of absolute cell counts after therapy. Patients in the poor PFS group (PFS < 6 months) compared to the favorable prognostic group (PFS ≥ 12 months) had significantly lower AUC for CD3+ T-cells ( $p = 0.0053$ ), CD4+ T-cells ( $p = 0.0026$ ), and NK-cells

( $p = 0.0008$ ) (Fig. 4). AUC of CD8+ T-cells, B-cells, eosinophils, and NLR were not different between the poor and good prognostic groups. To improve insight into potential relationships, we performed Spearman's correlation tests, revealing significant improvement of PFS (PFS < 6, ≥ 6 < 12, and ≥ 12 months) with increase in AUC of lymphocytes, total CD3+ T-cells, CD4+ T-cells, and NK-cells (Tab. S4).

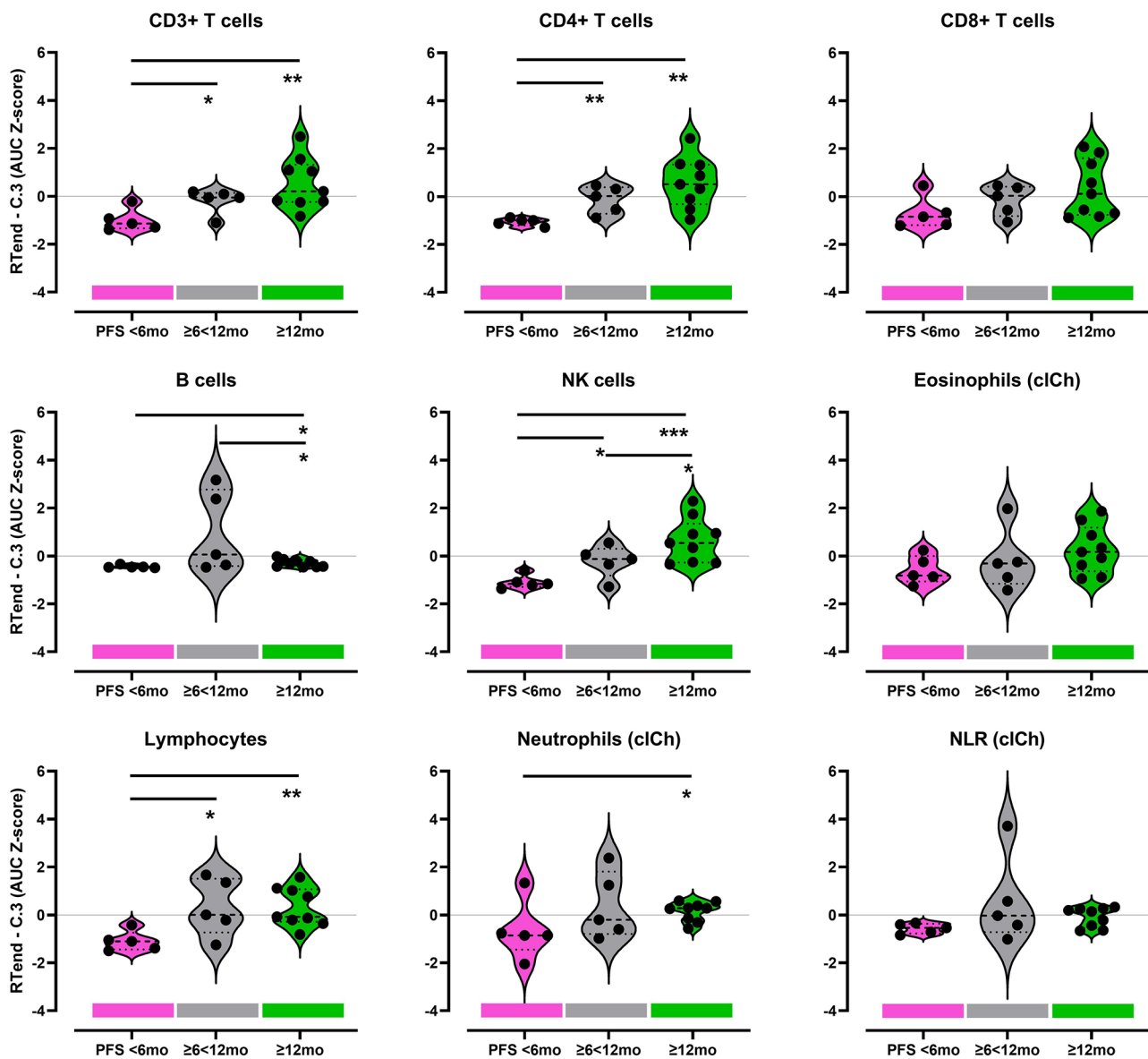


**Fig. 4** Standardized AUC (Z-score) for the interval RTend-C.3 of leukocyte subpopulations stratified according PFS groups (PFS < 6 months (red), PFS ≥ 6 < 12 months (grey), PFS ≥ 12 months (green)). Cell counts were derived from flow cytometry (gating strategy in Fig. S2), neutrophil, and eosinophil counts were determined by clinical chemistry routine lab (cICh). Each dot represents the value of an individual, bold dashed line in the violins indicate median, light dotted lines lower and upper quartile. For B-cells, p-value comparing PFS < 6 months to PFS ≥ 6 < 12 months was  $p = 0.0516$ . Student's T test, \*  $p < 0.05$ , \*\*  $p < 0.01$ , \*\*\*  $p < 0.001$

**Unsupervised clustering reveals longer PFS for patients receiving ICI**

Standardized lymphocyte parameters were clustered by unsupervised hierarchical clustering, which is an algorithm aiming to explain the relationship between all data points of a data set by clustering them with a distance according to their similarity. PFS, treatment regimen, local relapse, distant metastases were annotated to, but were not included in the clustering. The result (Fig. 5) identified two clusters: on the right side were patients with low AUC for all cell types, except NLR (assigned “cold” group) (9 of 19 patients). Only 1 patient (1 of 9 patients) within this group had received ICI.

Most patients (7 of 9 patients) in this “cold” lymphocyte-reduced group had developed local tumor recurrence (LR) after definitive therapy and only 2 (of 9) belonged to the favorable group (PFS ≥ 12 months). Patients clustering to the left (10 of 19 patients) had higher AUC (RTend-C.3) for all leukocyte subpopulations except NLR (assigned “hot” group). Six of the patients of the “hot” group had been treated with ICI (6 of 10), only 2 (of 10) had experienced LR and most belonged to the favorable PFS group (7 of 19).

Fisher’s Exact Testing “cold” or “hot” group against good or poor PFS (≥ 12 months 10 patients; and < 12 months, 9 patients, respectively) revealed a statistically

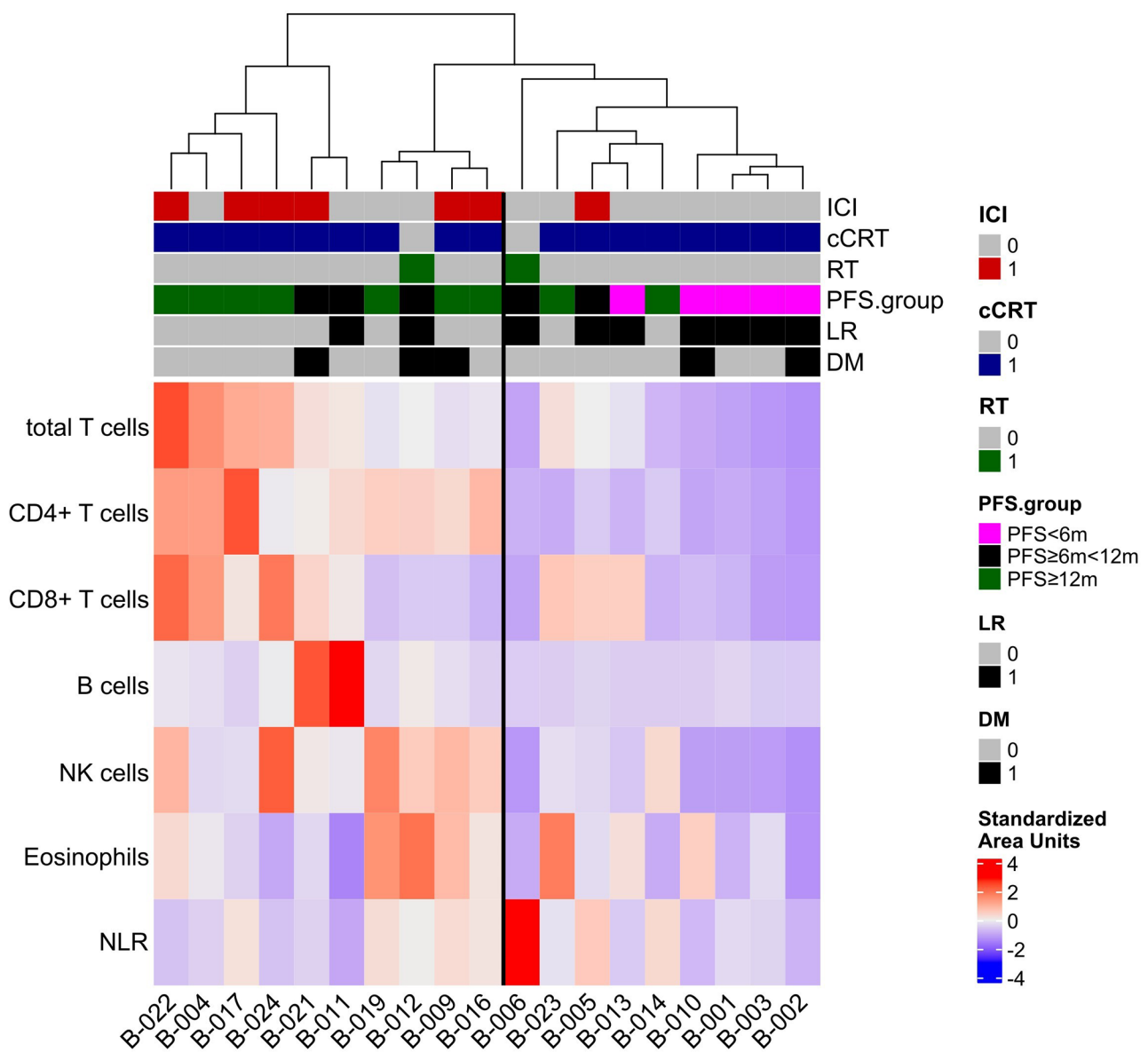


**Fig. 5** Heatmap of unsupervised clustering of AUC (RTend-C.3) of leukocyte subpopulations, PFS (< 6 months, ≥ 6 < 12 months, and ≥ 12 months), treatment regime and recurrence (LR, local recurrence; DM, distant metastases) (AUCs) in patients (n = 19). Bold vertical line separates a “hot” group (higher AUC) and a left “cold” group (lower AUC)

non-significant value of  $p=0.069$ . The Odds ratio (95% CI) was 7.17 (0.752, 113.47).

#### Linear discriminant analysis (LDA) of blood cell subpopulations separates patients according to PFS

LDA analysis is a dimensionality reduction and pattern recognition algorithm that aims to cluster the lymphocyte subpopulations to predict the differences of the PFS groups. Clustering aims to find the greatest differences of mean and lowest variation between the groups. We analyzed the AUC of cell counts (CD4+ and CD8+ T-cells, B-cells, CD56+CD3- NK-cells, eosinophils, neutrophils, and the NLR) at the RTend-C.3 interval as predictor variables for PFS, defined in 3 groups: PFS < 6 months,  $\geq 6 < 12$  months, and  $\geq 12$  months.

Discriminant markers for PFS  $\geq 12$  months (green area) were the AUCs of CD4+ T-cells, and CD56+ NK-cells (Fig. 6, Fig. S5). By these markers, 6 of 9 patients of the PFS  $\geq 12$  months group were correctly separated from the other PFS groups. Patients with intermediate PFS ( $\geq 6 < 12$  months) (grey area) were discriminated by AUCs of B-cells and NLR, with four of five individuals of this group separated correctly. The mean of prediction as a

measure for accuracy was 0.947 for linear discriminant analysis.

#### Variation in IL-6 concentration is correlated with PFS

IL-6 is a pro-inflammatory cytokine that plays an important role in innate immunity and is upregulated in sepsis [11], after trauma [12], and medical treatment, e.g. surgery [13]. Basal IL-6 levels highly vary inter-individually [14], thus a comparison of absolute values for IL-6 across individuals is difficult to interpret. We focused on the intra-individual variation of IL-6 concentrations (pg/ml) over at least 3 consecutive timepoints, starting at RTend until C.3 as a clinically sensible interval for survival prediction. The standard deviation of the IL-6 concentrations (pg/ml) during this interval ( $n=4$  blood samples each patient) was used as a measure of variation of the IL-6 level.

The favorable survival group had a median standard deviation (RTend-C.3) of 2.5 (range 0.7–6.6), the poor survival group 22.9 (range 2.3–175.7), and the intermediate group 8.8 (range 4.0–12.3). Thus, the IL-6 variation after RTend was significantly lower for the favorable PFS group and this significantly correlated with PFS ( $p=0.007$ , Fig. 7).

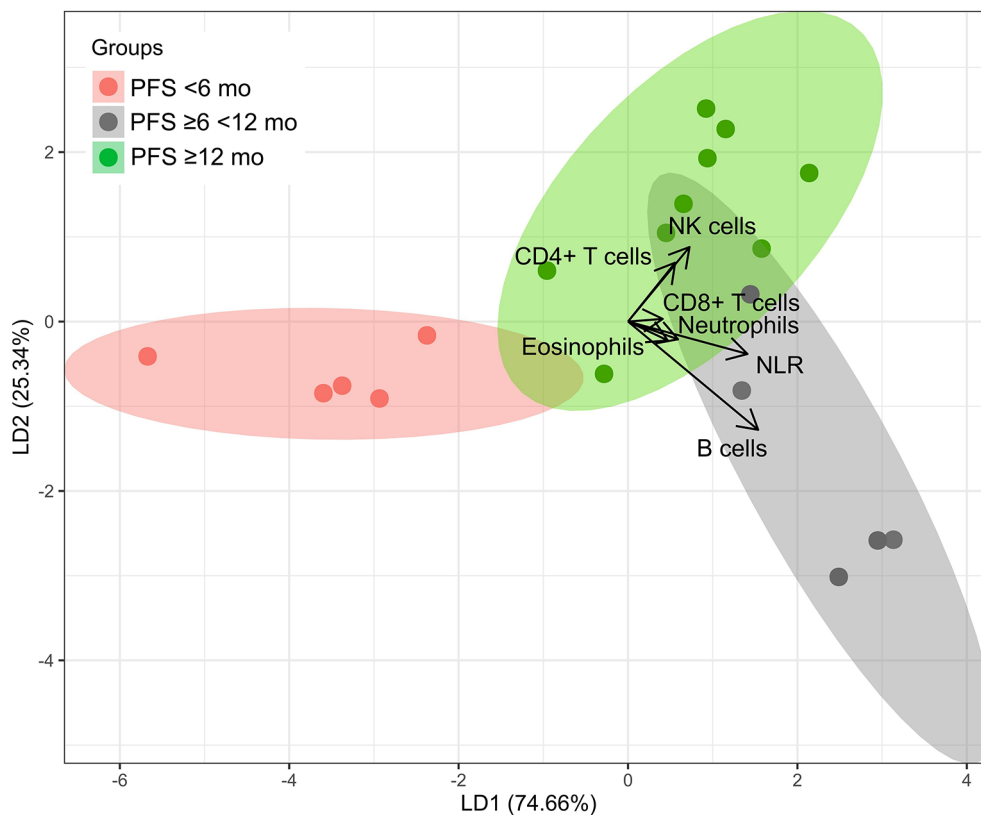


**Fig. 6** Linear discriminant analysis group plot (response variable PFS, predictor variables were AUCs of the interval RTend-C.3 of CD4+T-cells, CD8+T-cells, B-cells, NK-cells, eosinophils, neutrophils, and NLR). Mean as a measure for accuracy was 0.947. The length and direction of the arrows indicate how well the parameter differentiates this group from the others

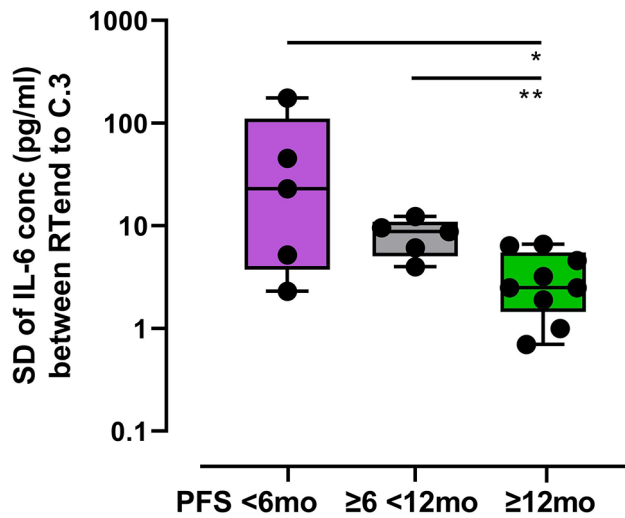


**Fig. 7** Standard deviation (SD) of IL-6 concentration from RTend-C.3 according to PFS groups (box plots showing median, min and max); Student's T test, \*  $p < 0.05$ , \*\*  $p < 0.01$

## Discussion

In this prospective explorative study, we evaluated the dynamics of defined peripheral leukocyte subsets in patients with inoperable stage II/III NSCLC during primary treatment and follow-up with the aim to identify peripheral T-cell subsets that may predict treatment outcome, especially PFS.

Our analysis provides evidence that ALC expansion after the end of definitive RT or cCRT until 6 months afterwards is significantly associated with treatment efficacy. Increase of AC in CD3+T-cells, CD8+cytotoxic T-cells, and NK-cells had the most pronounced effect and was associated with favorable PFS, whereas significant increase in B-cell counts had a less apparent positive association with PFS and eosinophils and CD4+T-cell counts had no association.

ALC before treatment (A.1) or at any other single timepoint did not reveal a correlation with PFS (Fig. 2). There was no significant correlation between ALC at six months after RTend and treatment regimen (data not shown).

Comparable to findings of previously published studies [5, 6, 15, 16] all patients in this study experienced moderate to severe lymphocytopenia during RT (A.2-RTend) with the nadir at the end of radiotherapy. Most of our patients recovered from lymphocytopenia within the following 3 (C.2) to 6 (C.3) mo. Some (4 of 16 at C.3) had persistently low cell counts (Fig. 2), which correlated with poor disease control with PFS less than 6 months (Fig. 4). An earlier study [17] found an association between severe lymphocytopenia ( $< 500$  cells/ $\mu$ l) and reduced OS (HR 1.70,  $p = 0.17$ ). Similar evidence was observed in glioblastoma [18], cervical cancer [19] and in seminoma [20]. This is comparable to what we see in this study, where

patients with continuously low ALC had poor PFS and OS (Fig. S3c, d).

In our study patients had favorable PFS and OS when treated with cCRT+ICI compared to cCRT alone (Fig. S3e, f). In a comparable investigation, Jing et al. [7] compared NSCLC patients who received cCRT with those who received additionally maintenance treatment with durvalumab. They found a significant increase in PFS in the durvalumab subgroup alongside with a significant correlation between lymphocytopenia and PFS/OS. Jing et al. observed no statistically significant evidence that patients with lymphocytopenia benefited from durvalumab in terms of improved overall survival. However, the authors focused on severe lymphocytopenia with a cell count of less than  $0.23 \cdot 10^9$  cells/L (230 cells/ $\mu$ l). Additional factors may play a role when ALC is extremely low. Our cohort was small and only five patients had very low ALC at the end of radiation. Of these patients, two received RT, one cCRT, and two received cCRT+ICI. Two cCRT+ICI patients showed a strong recovery of cell counts together with favorable PFS ( $\geq 23$  mo). Interestingly, Cho et al. [6] postulated that patients with severe lymphocytopenia may benefit most from additional ICI because a fresh and immunological potent lymphocyte population may arise from a depleted lymphocyte reservoir.

The time period following end of RT is considered to be significant since processes involving immunogenicity take place that play a role in durable immune activation and tumor rejection [21, 22]. In this study, we focused on the 6-mo period of RTend-C.3 and refer to it as a crucial recovery phase. Considering the different lymphocyte subtypes (Fig. 3, Fig. S4), we identified that an early increase in absolute counts after RT of total CD3+T-cells and CD8+T-cells was predictive of favorable PFS. Interestingly, Belka et al. [20] found that CD8+T-cells recovered significantly faster than CD4+T-cells after end of radiation treatment in patients with seminoma. In head and neck cancer, a gradual increase in CD8+T-cells over 6 months after radiotherapy was observed for non-recurrent patients [23]. This supports our finding that an early increase in CD8+T-cells in peripheral blood may be useful to predict favorable PFS. Kim et al. [24] reported on increasing frequency of Ki67+ cells within CD8+PD-1+T-cells in patients with locally advanced NSCLC during cCRT peaking at the last week during therapy followed by a decline 1-mo post-cCRT. These cells acquired a senescence phenotype. Although we did not include the Ki67 marker in this study we did not see a decline of CD8+T-cells but rather more CD8+T-cells in absolute counts from C.1.

We assumed that the dynamic changes of the cell counts may be meaningful for patient survival. Evidence that T-cell recovery is important was shown in a study

of melanoma patients by Huang et al. [22]. They found that a CD8+Ki67+ T-cell subpopulation positively correlated with clinical outcome when it peaked at a given early timepoint after therapy begin and subsequently decreased. To reflect the dynamic changes in absolute cell count in given subpopulations during the recovery interval of RTend-C.3, we calculate the AUC between four consecutive timepoints within 6 months after RT (RTend-C.1-C.2-C.3). This new approach can depict a broader picture of cellular dynamics in peripheral blood than the stepwise comparison of single timepoints. We identified that total lymphocytes and neutrophils, CD3+ T-cells, B-cells and NK-cells recover significantly faster and reach significantly higher AUC in patients with favorable PFS  $\geq 12$  months. Considering the T-cell subsets in this study, the prediction of long-term survival using this AUC method was statistically significant with the CD4+ but not with CD8+ T-cells.

We additionally used LDA as a classical approach in pattern recognition to define the cell subsets that contribute most to favorable outcome during the recovery phase (Fig. 6) [8, 9]. The LDA-approach allows to perform multiple linear correlations within one single statistical model. In addition to the cell subsets used before, we included neutrophil and eosinophil granulocytes, and neutrophil-leukocyte-ratio (NLR). A high value in AUC of CD4+ T-cells and NK-cells after RT end was found to correlate with a PFS  $\geq 12$  months. High AUC of CD4+ T-cells and NK-cells as well as addition of ICI contributed mostly to favorable PFS, and a trend of fewer local recurrences in these patients was detected. NLR as well as B-cells predicted a less favorable PFS of  $\geq 6 < 12$  months. This reiterates the literature where NLR has also been described as a marker for poor prognosis [25]. AUC of neutrophils and eosinophils had evidently only marginal predictive impact in our cohort.

For the ALC and AUC approaches, we observed different statistical associations with outcomes. This is due to the varying perspectives from which we analyzed the data. ALC analysis compares the single cell counts of each patient during recovery phase (RTend-C.3) within their PFS group. The focus is on identifying a subpopulation that potentially indicates favorable cell counts within the PFS groups at the earliest timepoint. For AUC analysis, cell counts at different time points are consolidated by a measure that reflects the dynamic changes during the selected time period, e.g., the RTend-C.3 recovery phase. This reduces dimensionality, allows for subpopulation comparisons between PFS groups, and identifies the blood cell population with the fastest recovery, that predicts favorable PFS. LDA analysis also represents a dimensionality reduction technique to uncover linear correlations between the cell data and the PFS groups. By

including more cell populations into the model, complexity increases, and may lead to different results. Results obtained by this approach can be considered robust when subpopulations have been identified as significant in more than one statistical model.

We also analyzed IL-6 plasma concentrations during and after treatment (Fig. 7). In in-vitro experiments using human NSCLC cancer cell lines as well as mouse models, Yamaji et al. [26] found an association between IL-6 and tumor proliferation. The pro-inflammatory cytokine IL-6 has predictive potential of severity in a variety of diseases, e.g. heart disease [27], pneumonia [28]. Absolute IL-6 values are challenging to compare across individuals because of interindividual differences as well as dependency on gender, sex, and age [29]. Therefore, we interrogated the intra-individual dynamics of IL-6 within a 6-mo period following RT/cCRT using the standard deviation as a measure for the magnitude of this variation. We found a strong negative correlation of IL-6 variation with PFS, which is consistent with the findings of Yamaji et al. [26].

The current study has limitations. It encompassed a small number of patients ( $n=20$ ) distributed over different treatment regimes. LDA may be problematic when used with small sample numbers [30] and when data deviate too much from normal distribution and homoscedasticity. To mitigate this issue, we interrogated a potential association with clinical benefit (OS, PFS) by various means including comparisons of single markers at individual timepoints or time intervals, as well as multi-parametric comparisons using unsupervised clustering and discriminatory analysis. Despite its limitations, our study has its value as it was conducted prospectively, and samples were collected longitudinally at multiple timepoints to characterize the recovery phase after RT. The results can be considered as a hypothesis to be tested in follow-up studies. If confirmed, the two identified parameters, peripheral CD8+ T-cell counts and IL-6 plasma concentration after treatment, are immediately amenable to clinical practice. A follow-up study is in progress including 40 inoperable stage III NSCLC patients [31].

## Conclusions

The present findings suggest that two parameters, which are commonly assessed in clinical routine, can be used to predict patient outcome. An early increase in CD8+ T cell lymphocyte count and low standard deviation in IL-6 plasma concentration are significantly correlated to patients with favorable, respectively poor outcome (PFS) after definitive therapy independent of treatment scheme. If confirmed, the two identified parameters are immediately amenable to clinical practice.

## Abbreviations

AB	Antibody
AC	Absolute Counts
ALC	Absolute Lymphocyte Count
ASP	Antibody Staining Panel
cCRT	concurrent Chemoradiotherapy
Durva	Durvalumab
FCM	Flow Cytometry
FCS	Fetal Calf Serum
FL	Fluorochrome
Gy	Gray
ICI	Immune Checkpoint Inhibition
IQR	Inter Quantile Range
LDA	Linear Discriminant Analysis
LQR	Lower Quartile Range
mo	Month(s)
Nivo	Nivolumab
NLR	Neutrophil-Lymphocyte-Ratio
NSCLC	Non Small Cell Lung Cancer
OS	Overall Survival
PFS	Progression-Free Survival
RT	Radiation Therapy
TRT	Thoracic Radiotherapy
UQR	Upper Quantile Range
y	Year(s)

## Supplementary Information

The online version contains supplementary material available at <https://doi.org/10.1186/s13014-025-02620-z>.

Supplementary Material 1

## Acknowledgements

We thank patients and their families, the clinicians and staff member of the LMU hospital, and colleagues at the Asklepios Fachkliniken München-Gauting. For excellent support, we thank Anna Herbstritt, Barbara Mosetter, and Adam Slusarski.

## Author contributions

TPH: conceptualization, methodology, data analysis, investigation, writing – original draft, visualization; AEN: methodology, data analysis, writing – review & editing, visualization; LK: resources, data curation; CJP: data curation; JT: resources, data curation; SM: data curation; CE: writing – review & editing; FM: conceptualization, supervision, writing – review & editing; EN: conceptualization, methodology, supervision, writing – review & editing.

## Funding

Open Access funding enabled and organized by Projekt DEAL.

## Data availability

The data that support the findings of this study are not openly available due to reasons of sensitivity and are available from the corresponding author upon reasonable request.

## Declarations

### Ethics approval and consent to participate

The study was approved by the Human Ethics Committee of the Ludwig-Maximilians-University of Munich reference no. 17–632 and conducted in accordance with the Declaration of Helsinki. Patients were included into the study after informed consent.

### Consent for publication

Not applicable.

### Competing interests

Lukas Kaesmann reports a relationship with AstraZeneca that includes: funding grants. Lukas Kaesmann reports a relationship with Amgen Europe GmbH that includes: speaking and lecture fees. Claus Belka reports a

relationship with Brainlab AG that includes: funding grants. Claus Belka reports a relationship with Elekta that includes: funding grants. Claus Belka reports a relationship with ViewRay Inc that includes: consulting or advisory, funding grants, speaking and lecture fees, and travel reimbursement. Claus Belka reports a relationship with Bristol Myers Squibb Co that includes: consulting or advisory, speaking and lecture fees, and travel reimbursement. Claus Belka reports a relationship with Roche that includes: consulting or advisory, speaking and lecture fees, and travel reimbursement. Claus Belka reports a relationship with Merck & Co Inc that includes: consulting or advisory, speaking and lecture fees, and travel reimbursement. Claus Belka reports a relationship with AstraZeneca that includes: consulting or advisory, speaking and lecture fees, and travel reimbursement. Claus Belka reports a relationship with European Society for Radiotherapy and Oncology that includes: board membership. Farkhad Manapov reports a relationship with AstraZeneca that includes: board membership, funding grants, and speaking and lecture fees. Farkhad Manapov reports a relationship with Novartis that includes: board membership and speaking and lecture fees. Farkhad Manapov reports a relationship with Roche that includes: speaking and lecture fees. Farkhad Manapov reports a relationship with Eli Lilly and Company that includes: speaking and lecture fees. Farkhad Manapov reports a relationship with Elekta that includes: speaking and lecture fees. Farkhad Manapov reports a relationship with Brainlab AG that includes: speaking and lecture fees. All other authors do not have any competing interests.

## Author details

<sup>1</sup>Helmholtz Zentrum München, Immunoanalytics – Tissue Control of Immunocytes, Munich, Germany

<sup>2</sup>Department of Radiation Oncology, LMU University Hospital, LMU Munich, Munich, Germany

<sup>3</sup>German Cancer Consortium (DKTK), Partner Site Munich, Munich, Germany

<sup>4</sup>Bavarian Cancer Research Center (BZKF), Munich, Germany

<sup>5</sup>Comprehensive Cancer Center, Munich, Germany

Received: 21 June 2024 / Accepted: 10 March 2025

Published online: 20 March 2025

## References

1. Goldstraw P, Chansky K, Crowley J, Rami-Porta R, Asamura H, Eberhardt WE, et al. The IASLC lung cancer staging project: proposals for revision of the TNM stage groupings in the forthcoming (Eighth) edition of the TNM classification for lung cancer. *J Thorac Oncol*. 2016;11(1):39–51.
2. Ribas A, Wolchok JD. Cancer immunotherapy using checkpoint blockade. *Science*. 2018;359(6382):1350–5.
3. Page DB, Postow MA, Callahan MK, Allison JP, Wolchok JD. Immune modulation in cancer with antibodies. *Annu Rev Med*. 2014;65:185–202.
4. Li S, Zhang C, Pang G, Wang P. Emerging Blood-Based biomarkers for predicting response to checkpoint immunotherapy in Non-Small-Cell lung cancer. *Front Immunol*. 2020;11:603157.
5. Chen NB, Xiong M, Zhou R, Zhou Y, Qiu B, Luo YF, et al. CT radiomics-based long-term survival prediction for locally advanced non-small cell lung cancer patients treated with concurrent chemoradiotherapy using features from tumor and tumor organismal environment. *Radiat Oncol*. 2022;17(1):184.
6. Cho Y, Kim Y, Chamseddine I, Lee WH, Kim HR, Lee JJ, et al. Lymphocyte dynamics during and after chemo-radiation correlate to dose and outcome in stage III NSCLC patients undergoing maintenance immunotherapy. *Radiation Oncol*. 2022;168:1–7.
7. Jing W, Xu T, Wu L, Lopez PB, Grassberger C, Ellsworth SG, et al. Severe Radiation-Induced lymphopenia attenuates the benefit of durvalumab after concurrent chemoradiotherapy for NSCLC. *JTO Clin Res Rep*. 2022;3(9):100391.
8. Ye J, Ji S. Discriminant analysis for dimensionality reduction: an overview of recent developments; in *biometrics: theory, methods, and applications*. New York: Wiley IEEE; 2009.
9. Zhao SP, Zhang B, Yang J, Zhou JH, Xu Y. Linear discriminant analysis. *Nat Rev Method Prime*. 2024;4(1).
10. Hammer O. PAST: paleontological statistics software package for education and data analysis. *Palaeontologia Electronica*. 2001;4(1).
11. Hack CE, De Groot ER, Felt-Bersma RJ, Nuijens JH, Van Strack RJ, Eerenberg-Belmer AJ, et al. Increased plasma levels of interleukin-6 in sepsis. *Blood*. 1989;74(5):1704–10.

12. Cuschieri J, Bulger E, Schaeffer V, Sakr S, Nathens AB, Hennessy L, et al. Early elevation in random plasma IL-6 after severe injury is associated with development of organ failure. *Shock*. 2010;34(4):346–51.
13. Cheng E, Shi Q, Shields AF, Nixon AB, Shergill AP, Ma C et al. Association of inflammatory biomarkers with survival among patients with stage III colon cancer. *JAMA Oncol*. 2023.
14. Said EA, Al-Reesi I, Al-Shizawi N, Jaju S, Al-Balushi MS, Koh CY, et al. Defining IL-6 levels in healthy individuals: A meta-analysis. *J Med Virol*. 2021;93(6):3915–24.
15. Zhang J, Huang SH, Li H, Li Y, Chen XL, Zhang WQ, et al. Preoperative lymphocyte count is a favorable prognostic factor of disease-free survival in non-small-cell lung cancer. *Med Oncol*. 2013;30(1):352.
16. Tang C, Liao Z, Gomez D, Levy L, Zhuang Y, Gebremichael RA, et al. Lymphopenia association with gross tumor volume and lung V5 and its effects on non-small cell lung cancer patient outcomes. *Int J Radiat Oncol Biol Phys*. 2014;89(5):1084–91.
17. Campian JL, Ye X, Brock M, Grossman SA. Treatment-related lymphopenia in patients with stage III non-small-cell lung cancer. *Cancer Invest*. 2013;31(3):183–8.
18. Mohan R, Liu AY, Brown PD, Mahajan A, Dinh J, Chung C, et al. Proton therapy reduces the likelihood of high-grade radiation-induced lymphopenia in glioblastoma patients: phase II randomized study of protons vs photons. *Neuro Oncol*. 2021;23(2):284–94.
19. van Meir H, Nout RA, Welters MJ, Loof NM, de Kam ML, van Ham JJ, et al. Impact of (chemo)radiotherapy on immune cell composition and function in cervical cancer patients. *Oncoimmunology*. 2017;6(2):e1267095.
20. Belka C, Ottinger H, Kreuzfelder E, Weinmann M, Lindemann M, Lepple-Wienhues A, et al. Impact of localized radiotherapy on blood immune cells counts and function in humans. *Radiother Oncol*. 1999;50(2):199–204.
21. Demaria S, Ng B, Devitt ML, Babb JS, Kawashima N, Liebes L, et al. Ionizing radiation Inhibition of distant untreated tumors (abscopal effect) is immune mediated. *Int J Radiat Oncol Biol Phys*. 2004;58(3):862–70.
22. Huang AC, Postow MA, Orlowski RJ, Mick R, Bengsch B, Manne S, et al. T-cell invigoration to tumour burden ratio associated with anti-PD-1 response. *Nature*. 2017;545(7652):60–5.
23. Niu M, Combs SE, Linge A, Krause M, Baumann M, Lohaus F, et al. Comparison of the composition of lymphocyte subpopulations in non-relapse and relapse patients with squamous cell carcinoma of the head and neck before, during radiochemotherapy and in the follow-up period: a multicenter prospective study of the German cancer consortium radiation oncology group (DKTK-ROG). *Radiat Oncol*. 2021;16(1):141.
24. Kim KH, Pyo H, Lee H, Oh D, Noh JM, Ahn YC, et al. Dynamics of Circulating immune cells during chemoradiotherapy in patients with Non-Small cell lung cancer support earlier administration of Anti-PD-1/PD-L1 therapy. *Int J Radiat Oncol Biol Phys*. 2022;113(2):415–25.
25. Templeton AJ, McNamara MG, Seruga B, Vera-Badillo FE, Aneja P, Ocana A, et al. Prognostic role of neutrophil-to-lymphocyte ratio in solid tumors: a systematic review and meta-analysis. *J Natl Cancer Inst*. 2014;106(6):dju124.
26. Yamaji H, Iizasa T, Koh E, Suzuki M, Otsuji M, Chang H, et al. Correlation between Interleukin 6 production and tumor proliferation in non-small cell lung cancer. *Cancer Immunol Immunother*. 2004;53(9):786–92.
27. Zhang WR, Garg AX, Coca SG, Devereaux PJ, Eikelboom J, Kavsak P, et al. Plasma IL-6 and IL-10 concentrations predict AKI and Long-Term mortality in adults after cardiac surgery. *J Am Soc Nephrol*. 2015;26(12):3123–32.
28. Woiciechowsky C, Schoning B, Cobanov J, Lanksch WR, Volk HD, Docke WD. Early IL-6 plasma concentrations correlate with severity of brain injury and pneumonia in brain-injured patients. *J Trauma*. 2002;52(2):339–45.
29. Wei J, Xu H, Davies JL, Hemmings GP. Increase of plasma IL-6 concentration with age in healthy subjects. *Life Sci*. 1992;51(25):1953–6.
30. Tharwat A, Gaber T, Ibrahim A, Hassanien AE. Linear discriminant analysis: A detailed tutorial. *Ai Commun*. 2017;30(2):169–90.
31. Kasmann L, Taugner J, Eze C, Nieto A, Pelikan C, Florsch B, et al. Prospective evaluation of immunological, molecular-genetic, image-based and microbial analyses to characterize tumor response and control in patients with unresectable stage III NSCLC treated with concurrent chemoradiotherapy followed by consolidation therapy with durvalumab (PRECISION): protocol for a prospective longitudinal biomarker study. *Transl Lung Cancer Res*. 2022;11(7):1503–9.

## Publisher's note

Springer Nature remains neutral with regard to jurisdictional claims in published maps and institutional affiliations.